Clarification of the role of key active site residues of glutathione transferase Zeta/maleylacetoacetate isomerase by a new spectrophotometric technique

Philip G. BOARD*[1], Matthew C. TAYLOR*, Marjorie COGGAN*, Michael W. PARKER†, Hoffman B. LANTUM‡ and M. W. ANDERS‡

*Molecular Genetics Group, John Curtin School of Medical Research, Australian National University, Canberra ACT 2601, Australia, †The Biota Structural Biology Laboratory, St. Vincent's Institute of Medical Research, 9 Princes Street, Fitzroy, Victoria 3065, Australia, and ‡Department of Pharmacology and Physiology, University of Rochester Medical Center, Rochester, New York 14642, U.S.A.

hGSTZ1-1 (human glutathione transferase Zeta 1-1) catalyses a range of glutathione-dependent reactions and plays an important role in the metabolism of tyrosine via its maleylacetoacetate isomerase activity. The crystal structure and sequence alignment of hGSTZ1 with other GSTs (glutathione transferases) focused attention on three highly conserved residues (Ser-14, Ser-15, Cys-16) as candidates for an important role in catalysis. Progress in the investigation of these residues has been limited by the absence of a convenient assay for kinetic analysis. In this study we have developed a new spectrophotometric assay with a novel substrate [(±)-2-bromo-3-(4-nitrophenyl)propionic acid]. The assay has been used to rapidly assess the potential catalytic role of several residues in the active site. Despite its less favourable orientation in the crystal structure, Ser-14 was the only residue found to be essential for catalysis. It is proposed that a conformational change may favourably reposition the hydroxyl of Ser-14 during the catalytic cycle. The $Cys^{16} \rightarrow Ala$ (Cys-16 mutated to Ala) mutation caused a dramatic increase in the K_m for glutathione, indicating that Cys-16 plays an important role in the binding and orientation of glutathione in the active site. Previous structural studies implicated Arg-175 in the orientation of α-halo acid substrates in the active site of hGSTZ1-1. Mutation of Arg-175 to Lys or Ala resulted in a significant lowering of the k_{cat} in the Ala-175 variant. This result is consistent with the proposal that the charged side chain of Arg-175 forms a salt bridge with the carboxylate of the α-halo acid substrates.

Key words: catalysis, glutathione transferase (GST), maleylacetate isomerase (MAAI), site-directed mutagenesis, spectrophotometry, Zeta-class glutathione transferase.

INTRODUCTION

GSTZ1-1 (glutathione S-transferase Zeta 1-1) is widely distributed in nature and is found in a range of species from mammals to insects, plants and fungi [1]. hGSTZ1-1 (human GSTZ1-1) is also known as maleylacetoacetate isomerase (MAAI, EC 5.2.1.2) and catalyses the glutathione-dependent isomerization of MAA (maleylacetoacetate) to FAA (fumarylacetoacetate), the penultimate step in the catabolism of tyrosine [2]. This is an important metabolic pathway, as deficiencies of its component enzymes are associated with severe disorders, such as phenylketonuria and hypertyrosinemia type I. The metabolic significance of this pathway may explain the conservation and expression of GSTZ throughout such a diverse evolutionary range. In previous studies, we have also shown that Zeta-class GSTs catalyse the biotransformation of a range of α-haloacids, including DCA (dichloroacetic acid), fluoroacetic acid, and 2-chloropropionate [3,4]. DCA is of considerable interest, because it is carcinogenic in rodents [5–8], and humans are exposed to DCA via the consumption of chlorinated drinking water and as a metabolite of trichloroacetic acid and chloral hydrate [9]. DCA promotes the metabolism of lactic acid via activation of the pyruvate dehydrogenase complex and is used clinically for the treatment of congenital lactic acidosis [10].

Although the three-dimensional structures of human and plant Zeta-class GSTs have been determined by X-ray crystallography [11,12], little is known about the residues that are involved in catalysis with the different substrates. Understanding the residues involved and the reaction mechanism is important for the rational design of selective inhibitors that may find use in the clinical treatment of hypertyrosinemia type I. In most other GST classes, the pK_a of the cysteine thiol group in enzyme-bound glutathione is reduced to around 6.5, and the thiolate anion is stabilized by a hydrogen bond from a tyrosine, serine, or arginine residue within the N-terminal domain [13–15]. Exceptions occur in the Omega- and Beta-class GSTs that have an active-site cysteine that can form a disulphide with glutathione [16,17]. The Zeta-class GSTs from a range of species contain a characteristic motif [SSCX(W/H)RVIAL, using one-letter symbols to denote amino acids] in the N-terminal region [1]. The first three residues of this motif line the active-site pocket. Each of these residues (Ser-14, Ser-15, Cys-16) could play a role in catalysis, and there are examples in other GSTs where different residues contribute to catalysis with different substrates. In addition, the crystal structure of hGSTZ1-1 contains a bound sulphate molecule that is co-ordinated by Arg-175 [11]. Molecular modelling suggests that Arg-175 forms a salt bridge with the carboxylate of α-haloacid substrates and plays a critical role in maintaining their correct orientation in the active site.

Progress in the investigation of active site residues and the reaction mechanism of the Zeta-class GSTs has been limited by the absence of a convenient assay for kinetic analysis. We have now developed and validated a new spectrophotometric assay with a novel α-haloacid substrate, BNPP [(±)-2-bromo-3-(4-nitrophenyl)propanoic acid]. This new method has been used to probe the active site and the reaction mechanism of hGSTZ1-1.

Abbreviations used: BCPP, 2-bromo-3-(4-chlorophenyl)propanoic acid; BNPP, (±)-2-bromo-3-(4-nitrophenyl)propanoic acid; CFA, chlorofluoroacetic acid; $Cys^{16} \rightarrow Ala$, Cys-16 mutated to Ala etc.; DCA, dichloroacetic acid; FA, fumarylacetone; FAA, fumarylacetoacetate; GS-CPP, 2-(glutathion-*S*-yl)-3-(4-chlorophenyl)propanoic acid; GS-NPP, 2-(glutathion-*S*-yl)-3-(4-nitrophenyl)propanoic acid; GST, glutathione transferase; hGSTZ1-1, human GST Zeta 1-1; MA, maleylacetone; SA, salicylic acid; TCHQ, tetrachlorohydroquinone.

[1] To whom correspondence should be addressed (e-mail philip.board@anu.edu.au).

EXPERIMENTAL

Materials

MA (maleylacetone), a surrogate substrate for MAA [18], was synthesized by a method described previously [19]. FA (fumarylacetone) was obtained from the Chemistry Centre (Perth, Australia). CFA (chlorofluoroacetic acid, 99 % pure) was prepared by hydrolysis of CFA ethyl ester (Lancaster Synthesis, Windham, NH, U.S.A.), as described previously [20]. BNPP was obtained from the Chemistry Centre (Perth, Australia).

Enzyme assays

Activity with DCA or CFA as substrates was determined by assaying the formation of glyoxylate, as described previously [4]. The isomerization of MA to FA was determined by a HPLC method modified from previously described procedures [21]. The reaction mixture contained 0.01 M sodium phosphate (pH 7.6), 500 μM glutathione, 500 μM MA, and 0.1–1.0 μg/ml enzyme in a final volume of 500 μl. The reaction was incubated at 25 °C and was stopped after 30 s by addition of 100 μl of ice-cold stop solution, which contained a 1:1 mixture of 1 M HCl and 5 μM SA (salicylic acid) as an internal standard. The samples were chilled to 4 °C and analysed by HPLC to determine the quantity of FA produced. MA, FA, and SA were separated on a Waters μBondapak C_{18} column (3.9 mm × 300 mm), eluted with a mobile phase at 1.5 ml/min. The mobile phase consisted of 40 % acetonitrile, 1 % triethylamine, 59 % MilliQ water. The pH of the mixture was brought to 3.1–3.2 with phosphoric acid, and the mixture was sparged with helium. The absorbance of the eluate was monitored at 312 nm. Under these conditions, the solvent peak eluted at 1.6 min, MA at 2.4 min, FA at 3.4 min, and the internal standard (SA) at 4 min. FA formation was quantified by reference to a standard curve prepared with pure FA. The concentration of MA used in these studies was determined by conversion of a sample of MA to FA in the presence of glutathione and hGSTZ1c-1c.

For the determination of kinetic constants, activities were determined in a 5 × 5 matrix of glutathione and MA concentrations. Glutathione concentrations ranged from 1–500 μM and MA concentrations ranged from 30–300 μM. The data were fitted to the Michaelis–Menten equation by MacCurveFit, version 1.1.2 (Kevin Raner, Mt Waverly, Victoria, Australia).

Spectrophotometric assay of GSTZ1-1 activity

Because the previously developed assays for GSTZ1-1 activity are cumbersome endpoint procedures, we developed a new method that allows the continuous spectrophotometric recording of enzyme activity, which simplifies the kinetic characterization of this enzyme. The method is based on the previously noted activity of GSTZ1-1with α-halopropionates [3]. Both BNPP and BCPP [2-bromo-3-(4-chlorophenyl)propanoic acid] were tested as substrates, but BNPP provided the greatest spectral change after conjugation with glutathione. The reaction mixture contained 0.1 M sodium phosphate buffer (pH 7.4), 1 mM glutathione, and 0.75 mM BNPP and was incubated at 37 °C. Because of the high absorbance of BNPP, it was necessary to use a dual-beam spectrophotometer with a blank reaction mixture that lacked enzyme in the reference cuvette.

Repetitive scanning of the reaction mixture between 400 and 250 nm revealed a maximum absorbance peak at 310 nm. The molar absorptivity of the reaction product GS-NPP [2-(glutathion-*S*-yl)-3-(4-nitrophenyl)propanoic acid] at 310 nm was 420. The pH optimum of the hGSTZ1-1-catalysed reaction of glutathione (1 mM) with BNPP (0.75 mM) as the substrate was determined with a range of buffers that have been described previously [22] for the characterization of glucose-6-phosphate dehydrogenase variants. The enzyme reaction rates were corrected for the non-enzymatic reaction rate at each pH. For the determination of kinetic constants, glutathione concentrations ranged from 0.05–1 mM and BNPP concentrations ranged from 0.025–0.5 mM. The data were fitted to the Michaelis–Menten equation by non-linear regression with MacCurveFit version 1.1.2.

LC-MS/MS analysis

Glutathione, substrates, and glutathione S-conjugates were analysed by tandem LC-MS/MS analysis with an Agilent 1100 Series LC/MSD-Trap SL controlled with the Agilent Chemstation software (version A.09.01) and the Agilent LC/MSD Trap 4.1 software (Agilent Technologies, Palo Alto, CA, U.S.A.). The instrument was equipped with a Nova-Pak®, 2.0 mm × 150 mm, C_{18}-column (Waters, Milford, MA, U.S.A.). The analytes were separated with a gradient mobile phase at a flow rate of 400 μl/min; solvent A: 10 mM ammonium formate (pH 3.2) was prepared in ultra-pure water (EM Sciences, Merck AG, Darmstadt, Germany); solvent B: 100 % HPLC-grade acetonitrile (J.T. Baker, Phillipsburg, NJ, U.S.A.). The gradient was as follows: 5 % solvent B for 2 min, increasing to 50 % solvent B over 5 min, and then held at 50 % solvent B for 3 min, with a total run time of 15 min.

MS/MS analyses were run in the positive APCI mode, and ionization conditions were optimized by continuous infusion of glutathione with a syringe pump. Interface conditions for optimal ionization were: dry-gas flow rate, 5.0 l/min; dry gas temperature, 350 °C; APCI temperature, 400 °C; nebulizer pressure, 60 psig; capillary voltage, 3270 V; capillary current; 95 nA; current end plate, 3314 nA; and corona current, 3931 nA. Conditions for the ion optics and CID trap were optimized with glutathione over the 50–600 *m/z* scan range; smart parameter settings were used for fragmentation in auto-MS/MS mode, and all ions of abundance greater than 10 000 were fragmented. Fragmentation voltages of 0.2, 0.6, and 1.0 V were used for manual MS/MS analysis. The MS/MS data were analysed with the data analysis software for version 4.1. The glutathione and the substrates were not retained on the column and eluted in the column dead volume. The retention times for GS-NPP and GS-CPP [2-(glutathion-*S*-yl)-3-(4-chlorophenyl)propanoic acid] were 8 and 9 min respectively. Both conjugates absorbed strongly at 254 nm.

Synthesis of GS-NPP and GS-CPP

Glutathione (0.36 mmol, 112 mg) (Sigma–Aldrich, St. Louis, MI, U.S.A.) was dissolved in 2 ml of ultra-pure water (EM Science, Merck KGaA, Darmstadt, Germany), and BNPP (0.18 mmol, 50 mg) or BCPP (0.18 mmol, 50 mg), dissolved in 1 ml of methanol, was added dropwise to the glutathione solution with stirring at room temperature; the final reaction volume was 3 ml. The pH of the solutions was brought to 9.0 with a few drops of 10 M NaOH. Product formation was monitored every 15 min by LC-MS/MS analysis, and the reaction was allowed to proceed to completion with stirring at room temperature for approx. 1 h. The reaction mixture was then concentrated under vacuum, and the dry

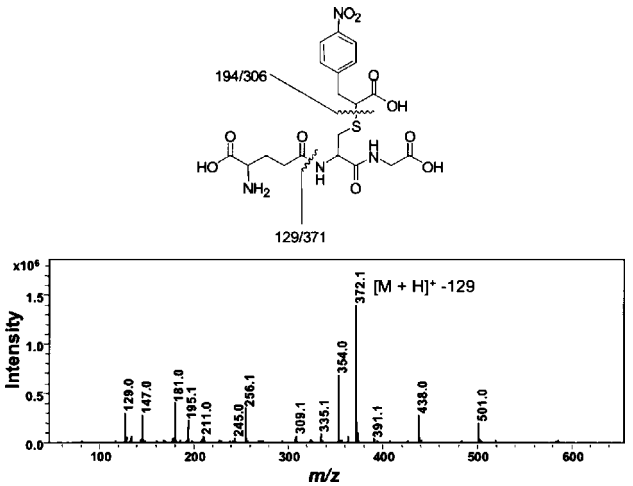

Figure 1 MS/MS analysis of GS-NPP

See Experimental section for details.

residue was taken up in 1 ml of 1 % acetic acid solution. Samples (3 μl) were analysed by LC-MS/MS.

Enzymatic synthesis of GS-NPP and GS-CPP

hGSTZ1b-1b (5 μg) was added to 950 μl of 0.1 M phosphate buffer (pH 7.4) containing 1 mM glutathione and incubated at 37 °C for 5 min. The reaction was started by addition of 50 μl of a 100 mM solution of either BNPP or BCPP in methanol. After incubation for 10 min at 37 °C, the reaction was stopped by addition of 50 μl of concentrated HCl, and 50 μl samples were used for analysis by LC-MS/MS.

Recombinant enzymes and mutagenesis

Recombinant variants of hGSTZ1-1 were expressed in *Escherichia coli* with an N-terminal poly-histidine fusion and purified as described previously [23]. Specific mutations were made with a QuickChange site-directed mutagenesis kit (Stratagene, La Jolla, CA, U.S.A.) and oligonucleotides obtained from Genset (Lismore, Australia). All mutations were made in the hGSTZ1c, the most common allelic variant, and each mutant cDNA was checked by DNA sequence analysis.

RESULTS

A new spectrophotometric assay

To facilitate the kinetic characterization of GSTZ1-1, we developed a novel spectrophotometric assay with BNPP as the substrate. During the development of this assay, we confirmed by LC-MS/MS that the hGSTZ1-1-catalysed conjugation of BNPP with glutathione gave GS-NPP (Figure 1). As observed with other α-halopropanoic acids [6], the α-bromo group of BNPP was displaced by glutathione to give GS-NPP. To determine if there was a spectral change associated with the formation of the GS-NPP, we recorded absorbance spectra between 400–250 nm of the hGSTZ1c-1c-catalysed reaction of glutathione with BNPP at 2 min intervals (Figure 2). The results showed that the greatest

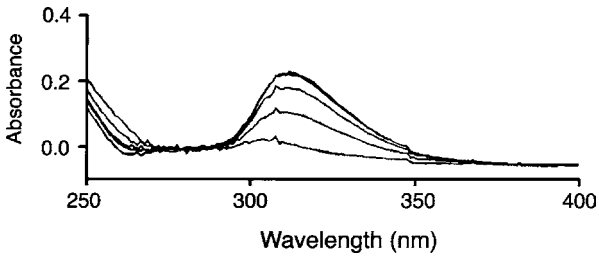

Figure 2 hGSTZ1-1-catalysed reaction of BNPP with glutathione

The reaction mixture contained glutathione (1 mM), BNPP (0.75 mM), and hGSTZ1c-1c and the spectra were recorded at 2 min intervals. The increase in absorbance at 310 nm indicates the formation of the reaction product GS-NPP.

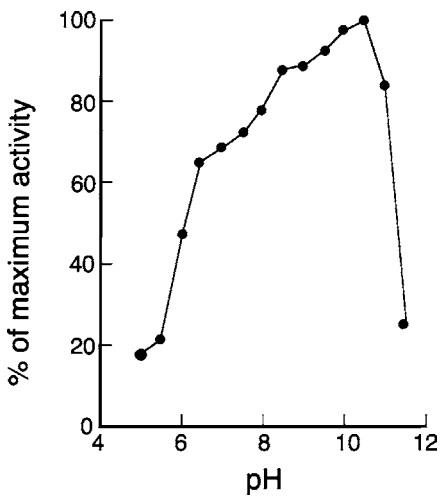

Figure 3 Effect of pH on the activity of hGSTZ1c-1c with BNPP as a substrate

Details of the buffers used have been described [22].

change in absorbance occurred at 310 nm. The molar absorptivity at 310 nm was 420. Because of the relatively low absorptivity of GS-NPP compared with BNPP, the assay lacks the sensitivity needed to determine GSTZ1-1 activity in crude tissue extracts. Nevertheless, the method allows the rapid determination of GSTZ1-1 activity in purified preparations. The optimum pH for the hGSTZ1c-1c-catalysed reaction of BNPP with glutathione was relatively broad with a peak at pH 10.5–11 (Figure 3). For subsequent kinetic analysis, a more physiological pH of 7.4 was used.

The specific activities of several naturally occurring allelic variants of hGSTZ1-1 are shown in Table 1. The rates obtained compare well with values obtained previously with other α-halo acids, including CFA. It is notable that among these naturally occurring variants, hGSTZ1a-1a has the highest activity and is significantly higher ($P = 0.0014$) than the value obtained for hGSTZ1c-1c, the most common variant. As shown in Table 1, the k_{cat} as well as the K_m^{BNPP} and K_m^{GSH} determined for hGSTZ1a-1a are all elevated in contrast to the other variants. In a previous study, we found that hGSTZ1a-1a shows selectivity between (*R*)- and (*S*)-2-chloropropionate [23]. The BNPP used in this study is a racemic modification, and the elevated activity of hGSTZ1a-1a may reflect a similar enantiomer selectivity.

Table 1 Specific activities and kinetic parameters of naturally occurring GST Zeta variants with BNPP and other α-halo acid substrates

Results are the mean ± S.D. of at least three determinations.

Enzyme	BNPP (μmol/min/mg)	CFA* (μmol/min/mg)	(*R*)-Z-Chloropropionate* (μmol/min/mg)	(*S*)-2-Chloropropionate* (μmol/min/mg)	k_{cat} (s^{-1})	K_m^{BNPP} (μM)	k_{cat}/K_m ($M^{-1} \cdot s^{-1}$)
hGSTZ1a-1a	2.3 ± 0.15	1.35 ± 0.05	1.11 ± 0.04	0.07 ± .002	1.3 ± .18	128 ± 43	10.2×10^3
hGSTZ1b-lb	1.5 ± 0.03	1.34 ± 0.03	0.28 ± 0.009	0.21 ± .004	0.82 ± .06	96 ± 19	8.5×10^3
hGSTZ1c-1c	1.6 ± 0.04	1.29 ± 0.05	0.29 ± 0.009	0.22 ± .005	0.59 ± .03	44 ± 8	13×10^3
hGSTZ1d-1d	1.2 ± 0.08	1.27 ± 0.025	0.26 ± 0.002	0.25 ± .004	0.55 ± .03	29 ± 7	19×10^3

* Data from reference [29].

Table 2 Specific activity and kinetic parameters for mutants of hGSTZ1-1 with CFA, BNPP and MA as substrates

Results are the mean ± S.D. for at least three determinations. ND, not detectable; S14A, $Ser^{14**} \rightarrow$ Ala mutant etc.

	Specific activity		BNPP				MA			
Enzyme	CFA (μmol/min/mg)	BNPP (μmol/min/mg)	k_{cat} (s^{-1})	K_m^{BNPP} (μM)	k_{cat}/K_m ($M^{-1} \cdot s^{-1}$)	K_m^{GSH} (μM)	k_{cat} (s^{-1})	K_m^{MA} (μM)	k_{cat}/K_m ($M^{-1} \cdot s^{-1}$)	K_m^{GSH} (μM)
hGSTZ1c-1c	0.91 ± 0.13	1.6 ± 0.04	0.56 ± 0.03	44 ± 7.6	1.3×10^4	134 ± 25	464 ± 64	347 ± 76	1.3×10^6	25 ± 5.8
S14A	0.007 ± 0.001	ND	ND	ND	ND	ND	ND	ND	ND	ND
S15A	0.025 ± 0.0004	2.7 ± 0.1	1.0 ± 0.14	319 ± 48	5.7×10^3	117 ± 25	72.6 ± 8.8	640 ± 120	1.1×10^5	14.6 ± 3.4
C16A	0.63 ± 0.03	3.7 ± 0.29	2.55 ± 0.4	417 ± 120	6.1×10^3	287 ± 34	141 ± 12	68 ± 14	2.1×10^6	298 ± 50
R175A	0.216 ± 0.003	0.45 ± 0.012	0.19 ± 0.01	23 ± 3.9	8.2×10^3	64 ± 16	149 ± 29	768 ± 190	1.9×10^5	13.9 ± 10
R175K	0.68 ± 0.04	1.41 ± 0.11	0.61 ± 0.027	27 ± 5.3	2.3×10^4	47 ± 16	368 ± 28	223 ± 31	1.7×10^6	17.8 ± 3.2

Mutagenesis of active site residues

Based on the crystal structure of hGSTZ1-1 and alignment of the sequences of other GSTs and related enzymes [1,11,24], we identified a number of residues that could potentially effect catalysis and substrate binding. Ser-14, Ser-15 and Cys-16 were considered the most likely to be involved in catalysis. These residues were mutated to alanine in hGSTZ1c. The specific activities of these mutant enzymes with different substrates are shown in Table 2. The $Ser^{14} \rightarrow$ Ala mutant was essentially inactive with all substrates and could not be subjected to further kinetic analysis. In contrast, the $Ser^{15} \rightarrow$ Ala mutant showed variable activity with different substrates when compared with hGSTZ1c-1c. Although the $Ser^{15} \rightarrow$ Ala mutant exhibited low isomerase activity with MA as a substrate ($\approx$15 % of wild-type) and low activity with CFA, it showed elevated activity with BNPP as the substrate. This elevated activity appears to be driven by a high k_{cat} and occurs despite an elevated K_m^{BNPP}.

The $Cys^{16} \rightarrow$ Ala mutant also showed variable activity with different substrates. This mutation diminished activity with both CFA and MA but showed significantly elevated activity with BNPP as a substrate. Again, this elevated activity appears to be driven by a high k_{cat}. In contrast, the diminished activity with MA appears to result from a low k_{cat}. It was notable that the $Cys^{16} \rightarrow$ Ala mutant had a very high K_m for glutathione in reactions with both BNPP and MA.

Examination of the crystal structure of hGSTZ1-1 indicated that Arg-175 may play a role in binding and orienting substrates in the active site [11]. To investigate this proposed role, we expressed $Arg^{175} \rightarrow$ Ala and $Arg^{175} \rightarrow$ Lys mutants and subjected them to kinetic analysis (Table 2). The importance of the positively charged side chain of Arg-175 is revealed by the lower specific activity and k_{cat} with BNPP and MA as substrates, as well as the elevated K_m for MA observed in the $Arg^{175} \rightarrow$ Ala mutant compared with the $Arg^{175} \rightarrow$ Lys and hGSTZ1c-1c (wild-type) variants.

DISCUSSION

Because of the cumbersome nature of the enzyme assays previously used to assay GSTZ1-1 activity with α-halo acids, we explored the possibility of developing a direct rate assay that could be easily followed spectrophotometrically. We tested both BNPP and BCPP as potential substrates, as we had shown previously that 2-chloropropionate was a substrate for hGSTZ1-1 and because we considered that the addition of a nitrophenyl or chlorophenyl substituent could provide a chromophore whose spectral properties would change after conjugation with glutathione. In preliminary studies, we found that BCPP showed negligible spectral changes after reaction with glutathione and hGSTZ1-1 and was not studied further. Our studies with BNPP confirmed that GSTZ1-1 catalysed the formation of the expected conjugate GS-NPP. The maximum change in absorbance occurred at 310 nm. Although this is a convenient wavelength for spectrophotometric studies, the change in molar absorptivity was low, which limits the sensitivity of the assay. Despite this limitation, the assay can be readily used to quantify the activity of purified GSTZ1-1. The optimal activity of hGSTZ1c-1c was relatively broad but had a peak at pH 10.5, which is considerably higher than the optimum with CFA as a substrate (pH 7.8–8.2) [25]; most other GSTs appear to have optima around pH 8.5 [13]. It was notable that among the naturally occurring allelic variants of hGSTZ1-1, we found that hGSTZ1a-1a had significantly higher activity with BNPP than the other variants. hGSTZ1a has an Arg residue in position 42 in comparison with a Gly in the other variants

[21]. We have previously reported that hGSTZ1a-1a is resistant to inactivation by DCA and shows high enantiomer selectivity with (*R*)-2-chloropropionate compared with (*S*)-2-chloropropionate [23,26]. It is possible that the elevated activity of hGSTZ1a-1a with BNPP may reflect similar enantiomer selectivity. The Arg or Gly residue at position 42 occurs at the tip of the so-called Mu loop region adjacent to helix α2 and together with helices α4 and α5 forms a gateway to the active site. The loop-α2 helix region is a mobile segment in the crystal structure [11], and it is possible that substitutions at this site modify the flexibility of the region. Such a change may modulate conformational changes required in converting between the apo, substrate bound, and product release states, thereby influencing catalysis with a variety of substrates.

The availability of this new direct spectrophotometric assay has facilitated the further investigation of critical residues involved in substrate binding and catalysis in the Zeta class GSTs. Alignment of Zeta class sequences with other members of the GST superfamily shows that Ser-14 in hGSTZ1 aligns with the active-site serine in mammalian Theta-class and insect Delta-class GST sequences and with Ser-11 in TCHQ (tetrachlorohydroquinone) dehalogenase from *Sphingomonas chlorophenolica* [1,4]. However, the crystal structure of hGSTZ1 suggests that the hydroxyl of Ser-14 is pointing away from the cysteinyl sulphur of glutathione and cannot form a hydrogen bond. In contrast, the crystal structure of hGSTZ1-1 indicates that the hydroxyl of Ser-15 is in a favourable position to form a hydrogen bond with the cysteinyl sulphur of enzyme-bound glutathione [11]. This suggests that Ser-15, rather than Ser-14, is likely to be a critical active-site residue. TCHQ dehalogenase catalyses the isomerization of MA to FA and appears to be phylogenetically related to the Zeta-class GSTs [24]. TCHQ dehalogenase has an active-site motif (Ser-11,Ile-12,Cys-13) that aligns well with the SSC motif in the Zeta-class GSTs, but lacks a Ser residue equivalent to Ser-15 in hGSTZ1. Nevertheless, Cys-13 appears to play a significant role in catalysis by TCHQ dehalogenase [27]. As well as being a substrate, DCA is a mechanism-based inactivator of rat and human Zeta-class GSTs [26]. In previous studies, we demonstrated that inactivation results from the covalent modification of Cys-16 by the *S*-(α-carboxymethyl)glutathione intermediate, which further implicates Cys-16 as a catalytically important residue [28]. Thus when all the available data are considered there is evidence implicating all three residues in the Zeta-class SSC motif as potential contributors to catalysis.

To evaluate the role of Ser-14, Ser-15 and Cys-16 in the Zeta-class motif as potential contributors to catalysis, we mutated each residue to alanine and examined the catalytic properties of each modified enzyme with CFA, BNPP and MA as substrates. Notably, there were some significant differences in the effects of each mutation with different substrates. The Ser-14 mutant was essentially inactive with each substrate tested. A molecular explanation for this loss of activity is not immediately clear. Our initial alignment of the hGSTZ1 sequence with other GSTs suggested that Ser-14 aligned with the active-site Ser-11 in the Theta-class GSTs and Ser-9 in the insect Delta class [1]. In the Theta- and Delta-class GSTs, the Ser-11/9 hydroxyl is positioned to form a hydrogen bond with the cysteinyl thiol of glutathione and contributes to the stabilization of bound glutathione as a thiolate and to catalysis [14,29–32]. The crystal structure of hGSTZ1 indicates that Ser-14 faces away from the thiol group of the bound glutathione, thus apparently precluding the formation of a hydrogen bond and a direct role in the stabilization of the thiolate [11]. Ser-14 is located at the N-terminal end of helix α1, and interacts with a residue from the preceding loop (main-chain atoms of Tyr-11) and a residue in the helix (main-chain and side-chain atoms of Ser-17). The former interactions appear to tether the loop to the helix. Mutation of Ser-14 to alanine would disrupt these interactions, possibly causing structural changes to the active site and increased thermal lability. In contrast, the crystal structure suggests that a hydrogen bond could possibly form between the hydroxyl of Ser-15 and the cysteinyl thiol of glutathione. The $Ser^{15} \rightarrow$ Ala mutant showed measurable activity with each substrate, but activity was substantially reduced with CFA and MAA and activity with BNPP was significantly greater than in hGSTZ1c-1c (wild-type). In an initial analysis, these data for Ser-14 and Ser-15 suggest that it is unlikely that the catalytic mechanism of the displacement or isomerization reactions is dependent on the stabilization of bound glutathione as a thiolate via a hydrogen bond from a serine residue as occurs in some other GSTs.

The role of Cys-16 was also probed by mutagenesis. The $Cys^{16} \rightarrow$ Ala mutant exhibited activity with each substrate. Although the MA isomerase activity was diminished, activity with BNPP was significantly elevated. This elevated activity appears to be driven by a high k_{cat} despite a very high K_m for glutathione. Although Copley and coworkers [24] have implicated the equivalent Cys residue in the MA isomerase activity of TCHQ dehalogenase, the present data indicate that, at least with the substrates studied here, Cys-16 plays a significant role in binding glutathione rather than a direct role in catalysis. The crystal structure of hGSTZ1-1 indicates that although the thiol groups of glutathione and Cys-16 are close (2.8 Å), they are not close enough to form a disulphide bond. Our previous studies show that Cys-16 is the primary nucleophile that reacts with the *S*-(α-carboxymethyl)glutathione carbonium-sulphonium intermediate that results in the inactivation of hGSTZ1-1 during the reaction with DCA [28]. Since the $Cys^{16} \rightarrow$ Ala mutant is active, it is clear that the thiol of Cys-16 is not required for catalysis in the reactions studied here, and it is likely that the inactivation that occurs with the formation of the Cys-16 adduct is based on steric hindrance. The cysteinyl thiol of glutathione is within hydrogen bonding or van der Waals distance of the amide of Cys-16 (3.5 Å) [11]; thus this interaction may be important for the binding and orientation of glutathione in the active site.

The crystal structure of hGSTZ1 indicates that the cysteinyl thiol of enzyme-bound glutathione is located almost directly over the N-terminal end of helix α1 [11]. The proximity of a Cys side chain to the positive end of a helix dipole has been shown to substantially lower the pK_a of the thiol [33]. The potential influence of a helix dipole on the activation of enzyme-bound glutathione and consequently on catalysis has been proposed in relation to other GSTs, and it is possible that it may also play a role in the Zeta-class GSTs [16,34].

Of the three potential catalytically active-site residues that we have investigated, the $Ser^{14} \rightarrow$ Ala mutation clearly had the greatest detrimental effect on activity. Thus despite its apparently inappropriate orientation in the active site, Ser-14 appears to be essential for catalysis. Although it is possible that this mutation caused a structural alteration that indirectly eliminated the enzyme's catalytic capacity, it is also possible that the active site undergoes a conformational change so that Ser-14 can interact with glutathione during the catalytic cycle. Such a change appears to occur in the Pi-class GSTs, where protonation of the bound glutathione causes a conformational change and loss of direct interaction of the catalytic tyrosine with glutathione [35]. In its protonated form, the thiol sulphur points in a different direction to that seen in other glutathione complexes. The crystal structure of the Zeta-class GST from *Arabidopsis thaliana* does not include glutathione and thus does not provide any further information in this regard [12]. The mutation of Ser-17 in the *A. thaliana* Zeta-class GST (equivalent to Ser-14 in hGSTZ1) reduces its

activity to $<2\%$ and $<6\%$ of the wild-type activity with DCA and MA respectively. Consequently, the available evidence indicates that Ser-14 or its equivalent may be of primary importance in catalysis with the currently known substrates of the Zeta-class GSTs. This is consistent with the mechanism proposed for the MAA isomerization reaction [12].

The crystal structure of hGSTZ1 indicated that Arg-175 may form a salt bridge with the carboxylate of α-haloacid substrates and may play a critical role in orientating the substrate so that glutathione can attack the α-carbon and displace the halide [11]. We evaluated this proposed role by constructing and expressing $Arg^{175} \rightarrow Ala$ and $Arg^{175} \rightarrow Lys$ mutants. The activity of the $Arg^{175} \rightarrow Ala$ mutant was significantly diminished with all substrates tested. In contrast, wild-type activities were largely maintained in the $Arg^{175} \rightarrow Lys$ mutant, thereby confirming the importance of the charged side chain. The k_{cat} and k_{cat}/K_m were lower in the $Arg^{175} \rightarrow Ala$ mutation for both the BNPP and MA isomerase reactions, again confirming the significance of Arg-175 in orientating the substrate. In addition, the K_m for MA was substantially elevated in the $Arg^{175} \rightarrow Ala$ mutant, which supports the contention that Arg-175 contributes to substrate binding and orientation. It is of interest that the K_m for glutathione for both the $Arg^{175} \rightarrow Ala$ and $Arg^{175} \rightarrow Lys$ mutants was reduced in reactions with both BNPP and MA, indicating that Arg-175 has an additional indirect influence on glutathione binding.

Concluding remarks

In this study, we have developed a new assay that has facilitated the exploration of the potential catalytic roles of several residues previously highlighted by structural studies of the Zeta-class GSTs. Although the enzyme has a range of catalytic activities, the displacement and isomerase reactions are dependent on the first of two conserved serine residues in the active site. Understanding the residues involved in catalysis and the reaction mechanisms will be of benefit in the design of inhibitors that could be used clinically to block the formation of FAA, a toxic intermediate in the tyrosine catabolic pathway. FAA accumulates in patients with FAA hydrolase deficiency (hypertyrosinemia type I) and is thought to be responsible for many of the severe consequences of this disorder [36]. This therapeutic possibility has increased in importance since the recent observation that $GSTZ1^{-/-}$ mice are not severely incapacitated [37].

We thank Kavitha Kugathas for technical assistance and Dr Dan Liu for assistance with the mutagenesis. This work was supported in part by grants from the National Health and Medical Research Council of Australia (P. G. B.), the Australian Research Council (M. W. P.), a National Health and Medical Research Council of Australia Senior Principal Research Fellowship (M. W. P.), and the National Institute of Environmental Health Sciences Grant ES03127 (M. W. A.)

REFERENCES

1 Board, P. G., Baker, R. T., Chelvanayagam, G. and Jermiin, L. S. (1997) Zeta, a novel class of glutathione transferases in a range of species from plants to humans. Biochem. J. **328**, 929–935
2 Fernandez-Canon, J. M. and Penalva, M. A. (1998) Characterization of a fungal maleylacetoacetate isomerase gene and identification of its human homologue. J. Biol. Chem. **273**, 329–337
3 Tong, Z., Board, P. G. and Anders, M. W. (1998) Glutathione transferase Zeta-catalyzed biotransformation of dichloroacetic acid and other alpha-haloacids. Chem. Res. Toxicol. **11**, 1332–1338
4 Tong, Z., Board, P. G. and Anders, M. W. (1998) Glutathione transferase Zeta catalyses the oxygenation of the carcinogen dichloroacetic acid to glyoxylic acid. Biochem. J. **331**, 371–374
5 Bull, R. J., Sanchez, I. M., Nelson, M. A., Larson, J. L. and Lansing, A. J. (1990) Liver tumor induction in B6C3F1 mice by dichloroacetate and trichloroacetate. Toxicology **63**, 341–359
6 DeAngelo, A. B., Daniel, F. B., Most, B. M. and Olson, G. R. (1996) The carcinogenicity of dichloroacetic acid in the male Fischer 344 rat. Toxicology **114**, 207–221
7 Harrington-Brock, K., Doerr, C. L. and Moore, M. M. (1998) Mutagenicity of three disinfection by-products: di- and trichloroacetic acid and chloral hydrate in L5178Y/TK +/− (−)3.7.2C mouse lymphoma cells. Mutat. Res. **413**, 265–276
8 Tao, L., Kramer, P. M., Ge, R. and Pereira, M. A. (1998) Effect of dichloroacetic acid and trichloroacetic acid on DNA methylation in liver and tumors of female B6C3F1 mice. Toxicol. Sci. **43**, 139–144
9 Krasner, S. W., McGuire, M. J., Jacangelo, J. G., Patania, N. L., Reagan, K. M. and Aieta, E. M. (1989) The occurence of disinfection by-products in U.S. drinking water. J. Am. Water Works Assoc. **81**, 41–53
10 Stacpoole, P. W., Henderson, G. N., Yan, Z. and James, M. O. (1998) Clinical pharmacology and toxicology of dichloroacetate. Environ. Health. Perspect. **106**, 989–994
11 Polekhina, G., Board, P. G., Blackburn, A. C. and Parker, M. W. (2001) Crystal structure of maleylacetoacetate isomerase/glutathione transferase Zeta reveals the molecular basis for its remarkable catalytic promiscuity. Biochemistry **40**, 1567–1576
12 Thom, R., Dixon, D. P., Edwards, R., Cole, D. J. and Lapthorn, A. J. (2001) The structure of a Zeta class glutathione S-transferase from *Arabidopsis thaliana*: characterisation of a GST with novel active-site architecture and a putative role in tyrosine catabolism. J. Mol. Biol. **308**, 949–962
13 Armstrong, R. N. (1997) Structure, catalytic mechanism, and evolution of the glutathione transferases. Chem. Res. Toxicol. **10**, 2–18
14 Caccuri, A. M., Antonini, G., Nicotra, M., Battistoni, A., Bello, M. L., Board, P. G., Parker, M. W. and Ricci, G. (1997) Catalytic mechanism and role of hydroxyl residues in the active site of theta class glutathione S-transferases. Investigation of Ser-9 and Tyr-113 in a glutathione S-transferase from the Australian sheep blowfly, *Lucilia cuprina*. J. Biol. Chem. **272**, 29681–29686
15 Bjornestedt, R., Stenberg, G., Widersten, M., Board, P. G., Sinning, I., Jones, T. A. and Mannervik, B. (1995) Functional significance of arginine 15 in the active site of human class α glutathione transferase A1-1. J. Mol. Biol. **247**, 765–773
16 Board, P. G., Coggan, M., Chelvanayagam, G., Easteal, S., Jermiin, L.S., Schulte, G. K., Danley, D. E., Hoth, L. R., Griffor, M. C., Kamath, A. V. et al. (2000) Identification, characterization and crystal structure of the Omega class glutathione transferases. J. Biol. Chem. **275**, 24798–24806
17 Rossjohn, J., Polekhina, G., Feil, S. C., Allocati, N., Masulli, M., De Illio, C. and Parker, M. W. (1998) A mixed disulfide bond in bacterial glutathione transferase: functional and evolutionary implications. Structure **6**, 721–734
18 Seltzer, S. (1973) Purification and properties of maleylacetone *cis*-trans isomerase from vibrio 01. J. Biol. Chem. **248**, 215–222
19 Fowler, J. and Seltzer, S. (1970) Synthesis of model compounds for maleylacetoacetic acid. J. Org. Chem. **35**, 3529–3532
20 Anderson, W. B., Board, P. G., Gargano, B. and Anders, M. W. (1999) Inactivation of glutathione transferase Zeta by dichloroacetic acid and other fluorine-lacking α-haloalkanoic acids. Chem. Res. Toxicol. **12**, 1144–1149
21 Polekhina, G., Board, P. G., Blackburn, A. C. and Parker, M. W. (2001) GSTZ1d: a new allele of glutathione transferase Zeta and maleylacetoacetate isomerase. Biochemistry **40**, 1567–1576
22 Beutler, E., Mathai, C. K. and Smith, J. E. (1968) Biochemical variants of glucose-6-phosphate dehydrogenase giving rise to congenital nonspherocytic hemolytic disease. Blood **31**, 131–150
23 Blackburn, A. C., Tzeng, H. F., Anders, M. W. and Board, P. G. (2000) Discovery of a functional polymorphism in human glutathione transferase Zeta by expressed sequence tag database analysis. Pharmacogenetics **10**, 49–57
24 Anandarajah, K., Kiefer, P. M., Jr., Donohoe, B. S. and Copley, S. D. (2000) Recruitment of a double bond isomerase to serve as a reductive dehalogenase during biodegradation of pentachlorophenol. Biochemistry **39**, 5303–5311
25 Lantum, H. B., Board, P. G. and Anders, M. W. (2002) Kinetics of the biotransformation of maleylacetone and chlorofluoroacetic acid by polymorphic variants of human glutathione transferase zeta (hGSTZ1-1). Chem. Res. Toxicol. **15**, 957–963
26 Tzeng, H. F., Blackburn, A. C., Board, P. G. and Anders, M. W. (2000) Polymorphism- and species-dependent inactivation of glutathione transferase Zeta by dichloroacetate. Chem. Res. Toxicol. **13**, 231–236
27 Kiefer, P. M., Jr. and Copley, S. D. (2002) Characterization of the initial steps in the reductive dehalogenation catalyzed by tetrachlorohydroquinone dehalogenase. Biochemistry **41**, 1315–1322

28 Anderson, W. B., Liebler, D. C., Board, P. G. and Anders, M. W. (2002) Mass spectral characterization of dichloroacetic acid-modified human glutathione transferase Zeta. Chem. Res. Toxicol. **15**, 1387–1397
29 Rossjohn, J., McKinstry, W. J., Oakley, A. J., Verger, D., Flanagan, J., Chelvanayagam, G., Tan, K. L., Board, P. G. and Parker, M. W. (1998) Human Theta class glutathione transferase: the crystal structure reveals a sulfate-binding pocket within a buried active site. Structure **6**, 309–322
30 Wilce, M. C., Board, P.G., Feil, S. C. and Parker, M. W. (1995) Crystal structure of a Theta-class glutathione transferase. EMBO J. **14**, 2133–2143
31 Tan, K. L., Chelvanayagam, G., Parker, M. W. and Board, P. G. (1996) Mutagenesis of the active site of the human Theta-class glutathione transferase GSTT2-2: catalysis with different substrates involves different residues. Biochem. J. **319**, 315–321
32 Jemth, P. and Mannervik, B. (2000) Active site serine promotes stabilization of the reactive glutathione thiolate in rat glutathione transferase T2-2. Evidence against proposed sulfatase activity of the corresponding human enzyme. J. Biol. Chem. **275**, 8618–8624
33 Kortemme, T. and Creighton, T. E. (1995) Ionisation of cysteine residues at the termini of model α-helical peptides. Relevance to unusual thiol p*K*a values in proteins of the thioredoxin family. J. Mol. Biol. **253**, 799–812
34 Sinning, I., Kleywegt, G. J., Cowan, S. W., Reinemer, P., Dirr, H. W., Huber, R., Gilliland, G. L., Armstrong, R. N., Ji, X., Board, P. G. et al. (1993) Structure determination and refinement of human Alpha class glutathione transferase A1-1, and a comparison with the Mu and Pi class enzymes. J. Mol. Biol. **232**, 192–212
35 Oakley, A. J., Bello, M. L., Battistoni, A., Ricci, G., Rossjohn, J., Villar, H. O. and Parker, M. W. (1997) Tyrosine and its catabolites: from disease to cancer. J. Mol. Biol. **274**, 84–100
36 Tanguay, R. M., Jorquera, R., Poudrier, J. and St-Louis, M. (1996) Tyrosine and its catabolites: from disease to cancer. Acta Biochim. Pol. **43**, 209–216
37 Fernandez-Canon, J. M., Baetscher, M. W., Finegold, M., Burlingame, T., Gibson, K. M. and Grompe, M. (2002) Maleylacetoacetate isomerase (MAAI/GSTZ)-deficient mice reveal a glutathione-dependent nonenzymatic bypass in tyrosine catabolism. Mol. Cell. Biol. **22**, 4943–4951

Received 28 April 2003/27 June 2003; accepted 10 July 2003
Published as BJ Immediate Publication 10 July 2003, DOI 10.1042/BJ20030625